# Dynamic Modeling of Tensegrity Robots Rolling over the Ground

### *Shinichi Hirai and Ryo Imuta

School Department of Robotics, Ritsumeikan University, Kusatsu, Shiga 525-8577, Japan

*Corresponding author: hirai@se.ritsumei.ac.jp

**Abstract**

This paper presents dynamic modeling of tensegrity robots rolling over the ground. We have developed a 6-strut tensegrity robot that deforms its body for rolling locomotion over the ground. Designing tensegrity structures and control laws appropriate to locomotion experimentally has consumed much time and labor. Dynamic simulation of tensegrity robot rolling is thus required to reduce time and labor in experimental trials.

We have formulated a set of dynamic equations of motion of tensegrity robots. Our tensegrity robots consist of rigid struts and elastic actuators. Elastic actuators, which act as tensile elements, shrink by applying air pressure into the actuators. Applying air pressure to designated actuators deforms the tensegrity structure, which allows the structure roll over the ground. We have simulated the rolling of two icosahedron tensegrity robots; one consists of 24 actuators while the other consists of 12 actuators. Experimental evaluation validated our dynamic simulation.

**Keywords** Tensegrity, Rolling, Dynamics, Modeling, Simulation

**Introduction**

Locomotion has been a main research issue in robotics and many robots have been proposed in the past decade including wheel robots, crawler robots, and legged robots. Recently, much attention has been paid to soft-bodied robots, which employ deformable bodies consisting of soft materials. Such soft-bodied robots can deform their body for locomotion. Deformable bodies are useful for obstacle avoidance and narrow passage locomotion. On the other hands, it is difficult to build larger bodies since soft materials deform naturally under gravity. To cope with this problem, we have proposed to introduce tensegrity structures into robot bodies.

Tensegrity structures consists of a set of rigid elements connected by elastic elements. Rigid elements, which are referred to as struts, act as bones of a robot while elastic elements, which are referred to as tensile elements, provide softness to the robot. Tenesgrity structures have been applied robot locomotion [Aldrich et al. (2003); Paul et al. (2006); Arsenault and Gosselin (2008)]. Most tensegrity robots employ crawling for locomotion. For dynamic locomotion, we have proposed tensegtity robots that roll over the ground [Shibata et al. (2009)] and developed a six-strut tensegrity robot driven by pneumatic McKibben actuators [Koizumi et al. (2012)]. Activating an appropriate set of actuators in sequence, a tensegrity robot rolls over the ground. Unfortunately, determining a sequence of appropriate actuators for locomotion requires much time since it is performed using a real robot in trial and error manner. Additionally, we have many choices in tensegrity structures. We have to select structures appropriate to rolling locomotion. This selection would require much time.

Determining actuator sequence and selecting tensegrity structures would be performed on a computer once we have establish a dynamic simulation of rolling tensegrity structures. Thus, we
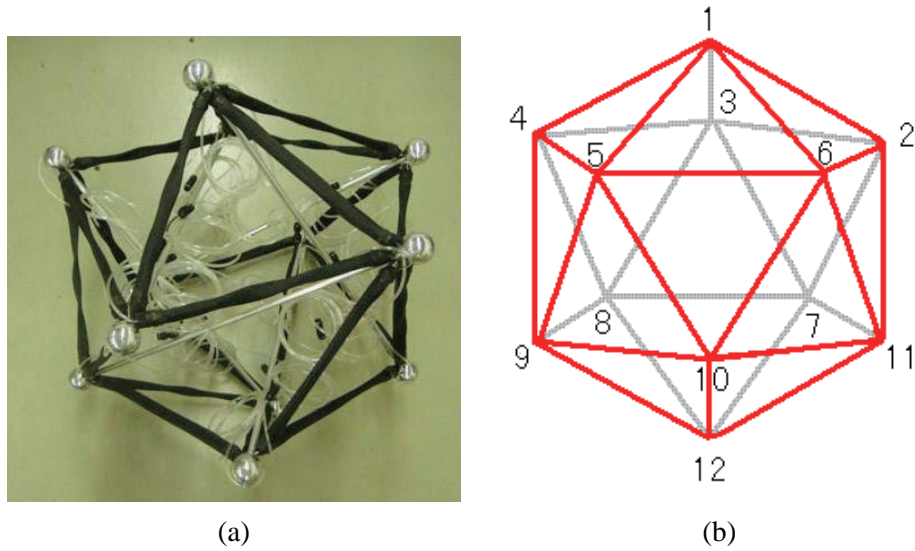
Figure 1: Prototype of six-strut tensegrity robot

will establish dynamic modeling of rolling tensegrity structures and perform simulation of rolling of tensegrity robots.

**Tesegrtity Robots**

Figure 1-(a) shows a prototype of six-strut tensegrity robots. This prototype consists of 6 rigid struts and 24 pneumatic McKibben actuators. The struts are made of aluminum and are 570 mm in length. Two rigid balls of diameter 45mm are attached to the both ends of each strut to help the rolling of a tensegrity robot. McKibben actuators shrink by applying air pressure and extend via external forces. Namely, McKibben actuators act as elastic elements. The actuators can generate force of 800 N at air pressure of 0.5MPa. Contraction ratio is almost 34% without load and 20% under the load of 3N by at air pressure of 0.5MPa. Air pressure to the actuators is applied externally through air hoses.

Figure 1-(b) shows geometric description of a six-strut tensegrity robot. Let us attach numbers 1 through 12 to individual vertices of the tensegrity robot. Then, each strut or each actuator is specified by a pair of numbers corresponding to its both ends. A six-strut tensegrity forms an icosahedron, consisting of eight regular triangles and twelve non-regular isosceles triangles. One triangle is contacting to the ground when this tensegrity robot is in equilibrium, implying that each equilibrium can be specified by its corresponding triangle.

Figure 2 describe successive rolling of a six-strut tensegrity robot. The prototype can perform a successive rolling over a flat ground by applying air pressure to a sequence of actuator pairs.

**Dynamic Modeling of Tensegrity Rolling**

Let us summarize the dynamic of a rigid body. Let us attach body coordinate system $\mathrm{C} - \xi\eta\zeta$ to the body while fix space coordinate system $\mathrm{O} - xyz$ to space. Orientation of a rigid body is described by rotation between the two coordinate systems. Let us introduce quaternion $\boldsymbol{q} = [\, q_0,\ q_1,\ q_2,\ q_3\,]^{\mathrm{T}}$ to describe the orientation of a rigid body [Kuipers 2002]. This quaternion must satisfy $\boldsymbol{q}^{\mathrm{T}}\boldsymbol{q} =$
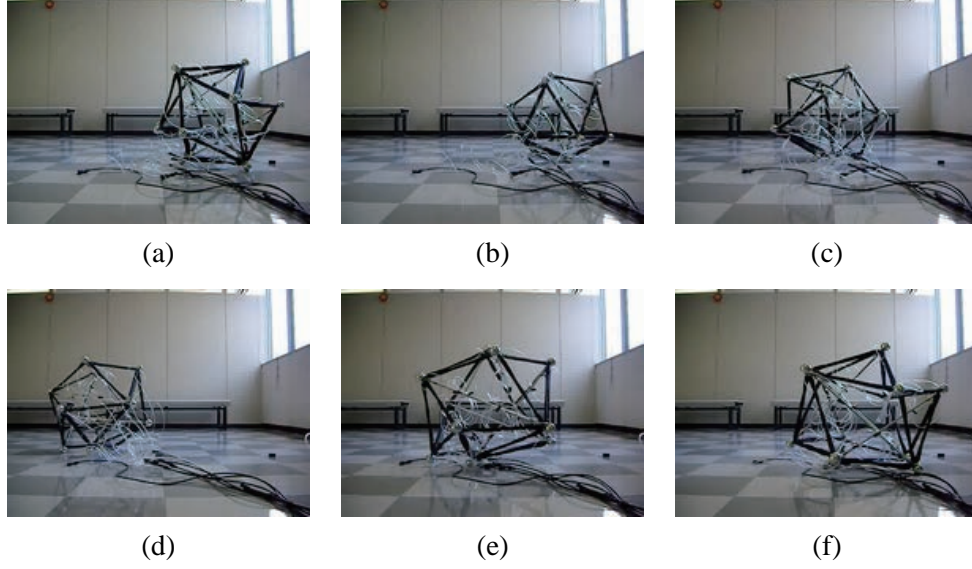
2

Figure 2: Successive rolling of a six-strut tensegrity robot

$q_0^2 + q_1^2 + q_2^2 + q_3^2 = 1$. The orientation matrix of a rigid body is then given as

$$R(\boldsymbol{q}) = \begin{bmatrix} 2(q_0^2 + q_1^2) - 1 & 2(q_1 q_2 - q_0 q_3) & 2(q_1 q_3 + q_0 q_2) \\ 2(q_1 q_2 + q_0 q_3) & 2(q_0^2 + q_2^2) - 1 & 2(q_2 q_3 - q_0 q_1) \\ 2(q_1 q_3 - q_0 q_2) & 2(q_2 q_3 + q_0 q_1) & 2(q_0^2 + q_3^2) - 1 \end{bmatrix}. \tag{1}$$

The first, second, and third columns of the above matrix correspond to unit vectors along $\xi$-, $\eta$-, and $\zeta$-axes. Angular velocity vector of a rigid body is described as

$$\boldsymbol{\omega} = 2H(\boldsymbol{q})\,\dot{\boldsymbol{q}} = -2H(\dot{\boldsymbol{q}})\,\boldsymbol{q}, \tag{2}$$

where

$$H(\boldsymbol{q}) = \begin{bmatrix} -q_1 & q_0 & q_3 & -q_2 \\ -q_2 & -q_3 & q_0 & q_1 \\ -q_3 & q_2 & -q_1 & q_0 \end{bmatrix}.$$

Let $J$ be inertia matrix of a rigid body and $\boldsymbol{\tau} = [\,\tau_\xi,\,\tau_\eta,\,\tau_\zeta\,]^{\mathrm{T}}$ be a set of external moments around $\xi$-, $\eta$-, and $\zeta$-axes applied to the body. Then, dynamic equation of rigid body rotation is formulated as:

$$\ddot{\boldsymbol{q}} = -r(\boldsymbol{q}, \dot{\boldsymbol{q}})\,\boldsymbol{q} - 2H^{\mathrm{T}}(\boldsymbol{q})\,J^{-1}\left( (H(\boldsymbol{q}\dot{\boldsymbol{q}}) \times (JH(\boldsymbol{q})\dot{\boldsymbol{q}}) - \frac{1}{4}\boldsymbol{\tau} \right), \tag{3}$$

where

$$r(\boldsymbol{q}, \dot{\boldsymbol{q}}) = \dot{\boldsymbol{q}}^{\mathrm{T}}\dot{\boldsymbol{q}} + 2\nu\boldsymbol{q}^{\mathrm{T}}\dot{\boldsymbol{q}} + \frac{1}{2}\nu^2(\boldsymbol{q}^{\mathrm{T}}\boldsymbol{q} - 1) \tag{4}$$

with positive constant $\nu$. This $r(\boldsymbol{q}, \dot{\boldsymbol{q}})$ originates from stabilization of holonomic constraint $\boldsymbol{q}^{\mathrm{T}}\boldsymbol{q} - 1 = 0$ [Baumgarte (1972)]. Denoting the right hand of Eq.3 by $\boldsymbol{h}(\boldsymbol{q}, \dot{\boldsymbol{q}}, \boldsymbol{\tau})$, dynamic equation of rigid body rotation is simply described as $\ddot{\boldsymbol{q}} = \boldsymbol{h}(\boldsymbol{q}, \dot{\boldsymbol{q}}, \boldsymbol{\tau})$.
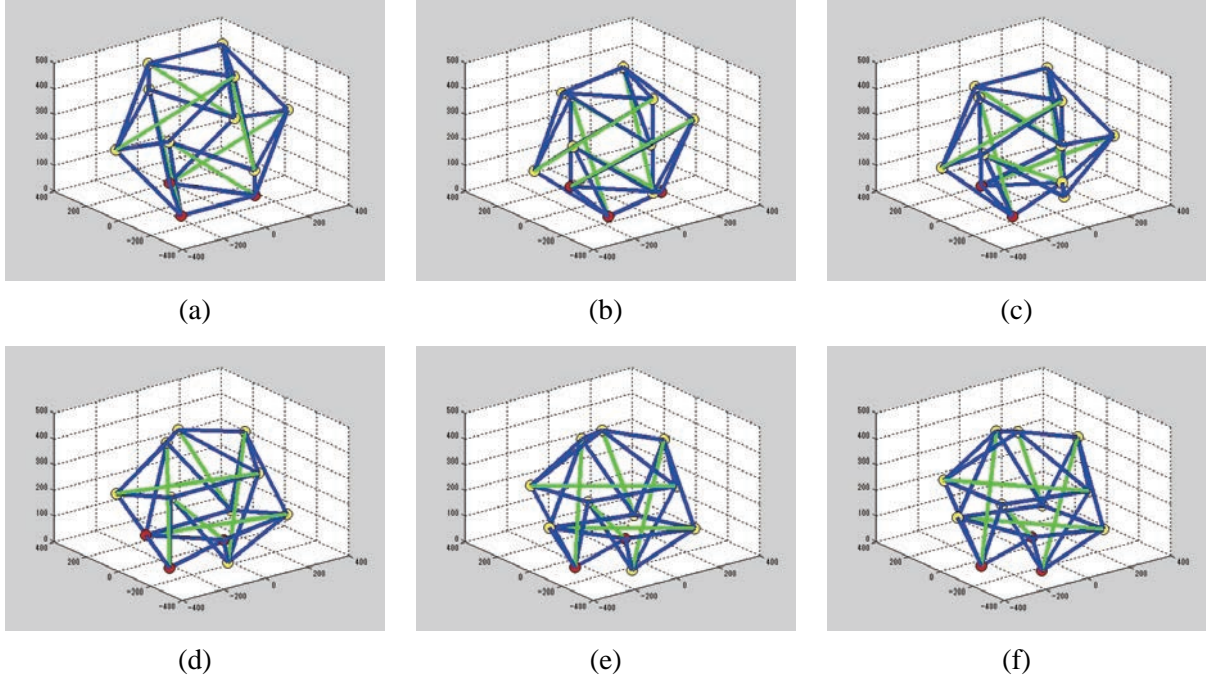
3

Figure 3: Simulation result of rolling of six-strut tensegrity robot

Let us formulate the motion of the $i$-th strut. Let $2L$ be the length of the struts. Assume that each strut is uniform with its mass $m$ and inertia matrix $J$. Let $C_i$ be the center of motion of the $i$-th strut and $x_i$ denote its position. Let us attach coordinate system $C_i - \xi_i \eta_i \zeta_i$ to the $i$-th strut. Assume that $\zeta_i$-axis lies on the line between the both end of the strut and $\boldsymbol{\zeta}_i$ be unit vector along $\zeta_i$-axis. Letting $\boldsymbol{f}_i$ and $\boldsymbol{\tau}_i$ be external force and moment applied to the $i$-th strut, equations of motion of the strut are given by

$$m\ddot{\boldsymbol{x}}_i = \boldsymbol{f}_i, \qquad \ddot{\boldsymbol{q}}_i = \boldsymbol{h}(\boldsymbol{q}_i, \dot{\boldsymbol{q}}_i, \boldsymbol{\tau}_i). \tag{5}$$

Recall that vertices of a six-strut tensegrity robot have their own numbers. Let $R_l$ be a set of numbers adjacent to vertex $l$ via elastic elements. Let $\boldsymbol{y}_l$ be the position vector of vertex $l$. Let $j$ and $k$ be vertex numbers at both end points of the $i$-th strut. Position vectors of the points are given by $\boldsymbol{y}_j = \boldsymbol{x}_i + L\boldsymbol{\zeta}_i$ and $\boldsymbol{y}_k = \boldsymbol{x}_i - L\boldsymbol{\zeta}_i$. Let $\boldsymbol{f}_{\mathrm{ela}}(\boldsymbol{y}_l, \boldsymbol{y}_n, \dot{\boldsymbol{y}}_l, \dot{\boldsymbol{y}}_n)$ be viscoelastic force generated by an elastic element connecting vertices $l$ and $n$. Then, the resultant force applied to vertex $j$ is formulated as

$$\boldsymbol{f}_i^+ = \sum_{l \in R_j} \boldsymbol{f}_{\mathrm{ela}}(\boldsymbol{y}_j, \boldsymbol{y}_l, \dot{\boldsymbol{y}}_j, \dot{\boldsymbol{y}}_l). \tag{6}$$

Similarly, the resultant force applied to vertex $k$ is given by

$$\boldsymbol{f}_i^- = \sum_{l \in R_k} \boldsymbol{f}_{\mathrm{ela}}(\boldsymbol{y}_k, \boldsymbol{y}_l, \dot{\boldsymbol{y}}_k, \dot{\boldsymbol{y}}_l). \tag{7}$$

Additionally, we will apply penalty method to formulate contact forces from the ground. Assuming that the ground is specified by $z \leq 0$, contact force applied to a vertex of which position is
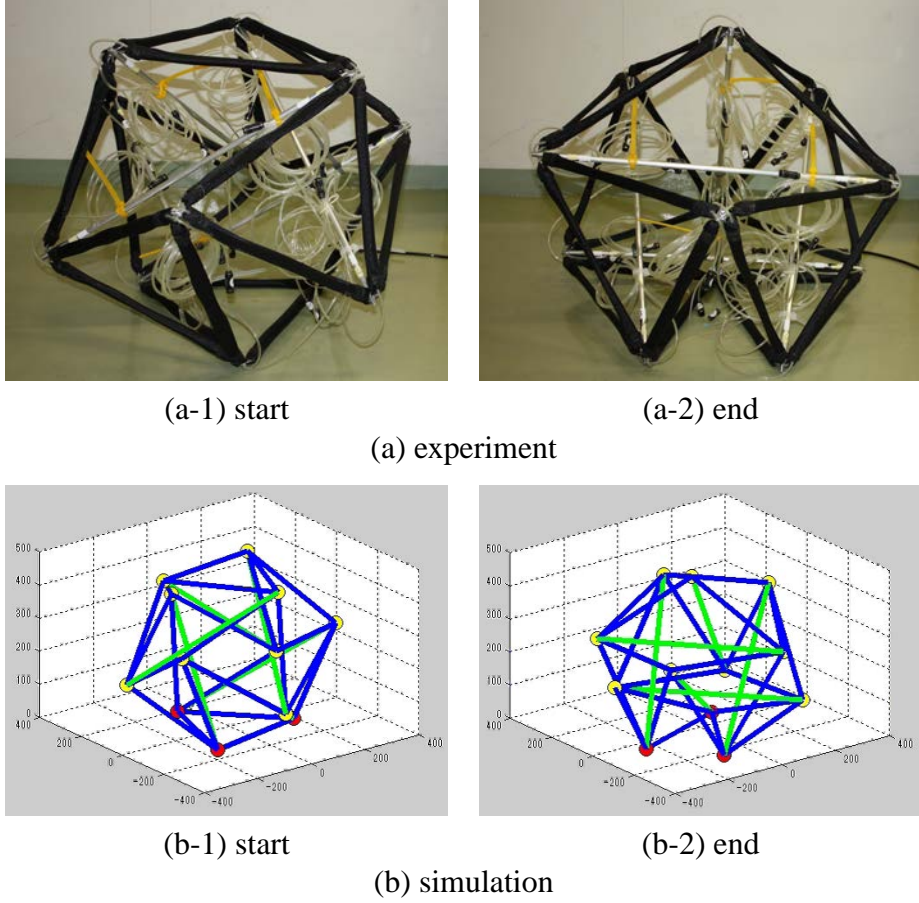
4

(a-1) start             (a-2) end

(a) experiment



(b-1) start             (b-2) end

(b) simulation

Figure 4: Six-strut tensegrity robot rolling from planar symmetric contact

represented as $\boldsymbol{x} = [\, x,\, y,\, z\,]^{\mathrm{T}}$ is given by

$$
\boldsymbol{f}_{\mathrm{con}}(\boldsymbol{x}) = \left\{ \begin{array}{cc} 0 & (z > 0) \\ -Kz - C\dot{z} & (z \le 0) \end{array} \right. ,
\tag{8}
$$

where $K$ and $C$ represent elastic and viscous coefficients of the ground. Contact forces applied to vertices $j$ and $k$ is then formulated as $\boldsymbol{f}_{\mathrm{con}}(\boldsymbol{y}_j)$ and $\boldsymbol{f}_{\mathrm{con}}(\boldsymbol{y}_k)$.

Consequently, the resultant force and moment applied to the $i$-th strut are formulated as:

$$
\boldsymbol{f}_i = \boldsymbol{f}_i^+ + \boldsymbol{f}_i^- + \boldsymbol{f}_{\mathrm{con}}(\boldsymbol{y}_j) + \boldsymbol{f}_{\mathrm{con}}(\boldsymbol{y}_k) + m\boldsymbol{g},
\tag{9}
$$

$$
\boldsymbol{\tau}_i = (L\boldsymbol{\zeta}_i) \times \left( \boldsymbol{f}_i^+ - \boldsymbol{f}_i^- + \boldsymbol{f}_{\mathrm{con}}(\boldsymbol{y}_j) - \boldsymbol{f}_{\mathrm{con}}(\boldsymbol{y}_k) \right),
\tag{10}
$$

where $\boldsymbol{g}$ represents the acceleration of gravity. Solving equations of motion of all struts numerically, we can simulate the motion and deformation of a tensegrity robot.

**Simulation Results**

We have performed dynamic simulation of rolling of a six-strut tensegrity robot. Figure 3 shows a sequence of snapshots of a result. Red circles describe vertices contacting to the ground while yellow ones are not in contact with the ground. At first, a regular triangle is in contact with the ground (Figure 3-(a)). Then, the body deforms (Figure 3-(b)) and one vertex of the regular triangle

5

(a-1) start            (a-2) end

(a) experiment



(b-1) start            (b-2) end
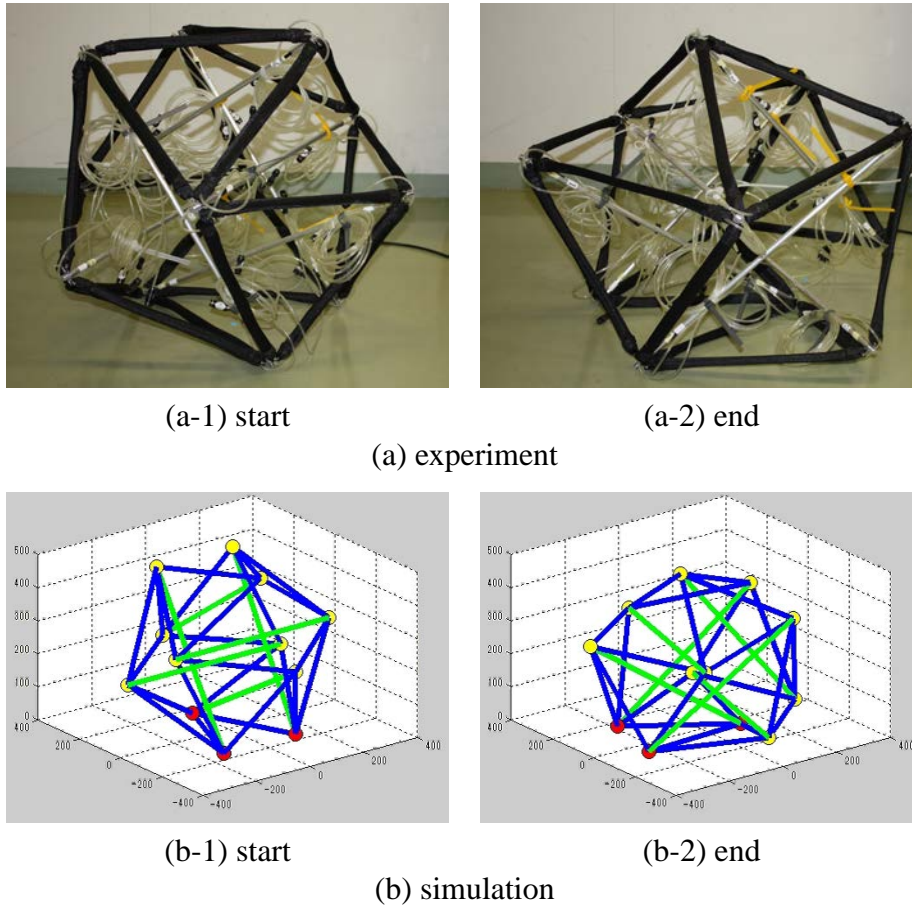
(b) simulation

Figure 5: Six-strut tensegrity robot rolling from planar symmetric contact

loses its contact (Figure 3-(c)). Namely, the tensegrity robot is out of equilibrium, yielding rotation around the line between the two contacting points (Figure 3-(d) and (e)). Finally, one vertex contacts to the ground, resulting that a non-regular isosceles triangle is in contact with the ground (Figure 3-(f)).

Contact between a six-strut tensegrity robot and the ground can be specified by the triangle contacting to the ground. Contact specified by a regular triangle is referred to as *axial symmetric contact* while contact represented by a non-regular isosceles triangles is referred to as *planar symmetric contact*. Note that we have eight axial symmetric contacts and twelve planar symmetric contacts. Rolling of a six-strut tensegrity robot corresponds to a sequence of transitions among the twenty contacts.

We have found that driving a pair of pneumatic McKibben actuators yields 1) transition from axial symmetric contact to its neighboring planar symmetric contact, or 2) transition from planar symmetric contact to its neighboring planar symmetric contact [Koizumi et al. (2012)]. Let us examine if the above two transitions can be simulated. Figure 4 shows experimental and simulation results of transition from axial to planar symmetric contacts. We have found that experimental and simulation results meet well. Figure 5 shows experimental and simulation results of transition from planar contact to its neighboring planar symmetric contact. The simulation result agrees with the experimental result. As a result, we conclude that dynamic simulation of rolling tensegrity robots works well.
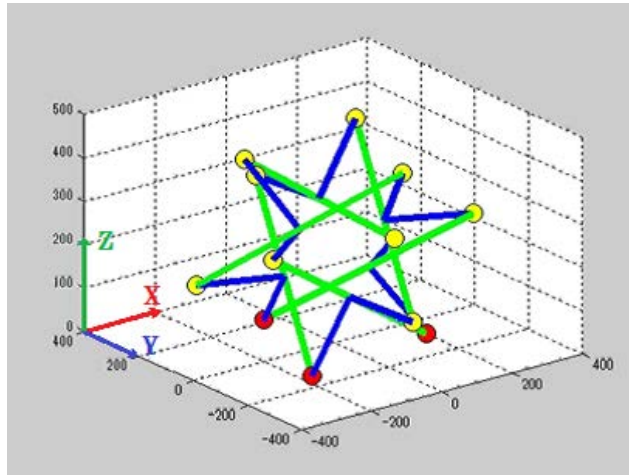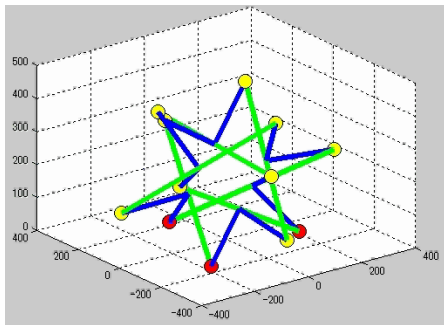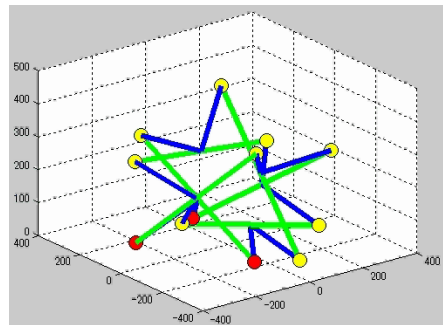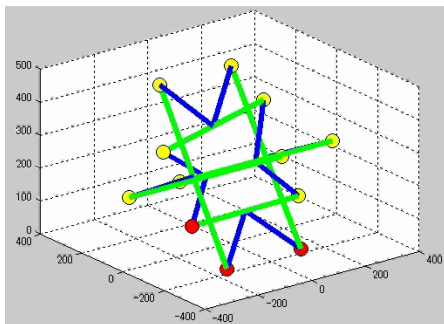
Figure 6: Star-shaped tensegrity robot
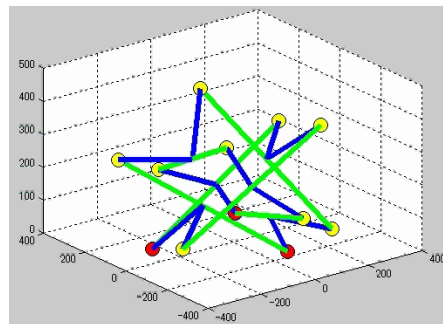


(a-1) start

(a-2) end

(a) transition from axial symmetric contact



(b-1) start

(b-2) end

(b) transition from planar symmetric contact

Figure 7: Simulation results of rolling of star-shaped tensegrity robot

Let us simulate the rolling of another tensegrity structure. Figure 6 shows a star-shaped tensegrity structure. This structure consists of six struts and twelve actuators. Each actuator connects one end point of a strut and the center of another strut. Note that no actuators contact to the ground during rolling. We have simulated transitions from axial and planar symmetric contacts. Figure 7 shows simulation results. Figure 7-(a) shows an axial symmetric contact transits to its neighboring planar symmetric contact. Figure 7-(b) describes a planar symmetric contact transits to its neighboring axial symmetric contact. These results suggest that this star-shaped tensegrity robot can perform rolling from any contact to another.

**Conclusion**

We have established dynamic simulation of tensegrity robot rolling. It turns out that rolling of a six-strut tensegrity robot can be simulated and simulation results agree with experimental results. Additionally, we have simulated the rolling of a star-shaped tensegrity robot. Through simulation, we have found that this tensegrity robot can perform rolling locomotion.

**References**

Aldrich, J. B., Skelton, R. E., and Kreutz-Delgado, K. (2003) Control Synthesis for a Class of Light and Agile Robotic Tensegrity Structures, Proc. American Control Conference, pp. 5245–5251.

Paul, C., Valero-Cuevas, F. J., and Lipson, H. (2006) Design and Control of Tensegrity Robots for Locomotion, *IEEE Trans. on Robotics*, Vol. 22, No. 5, pp.944–957.

Arsenault M. and Gosselin, C. M. (2008) Kinematic and Static Analysis of a Three-degree-of-freedom Spatial Modular Tensegrity Mechanism, *Int. Journal of Robotics Research*, Vol. 27, No. 8, pp.951–966.

Shibata, M. Saijyo, F. and Hirai, S. (2009) Crawling by Body Deformation of Tensegrity Structure Robots, *Proc. IEEE Int. Conf. on Robotics and Automation*, pp.4375–4380, Kobe, May 12–17.

Koizumi, Y., Shibata, M., and Hirai, S. (2012) Rolling Tensegrity Driven by Pneumatic Soft Actuators, *Proc. IEEE Int. Conf. on Robotics and Automation*, pp.1988–1993, St. Paul, U.S.A., May 14–18.

Kuipers, J. B. (2002) Quaternions and Rotation Sequences, Princeton University Press.

Baumgarte, J. (1972) Stabilization of constraints and integrals of motion in dynamical systems, *Computer Methods in Applied Mechanics and Engineering*, 1:1–16, .